

# Long-distance Bell-type tests using energy-time entangled photons

W.Tittel, J.Brendel, N.Gisin, and H.Zbinden

*University of Geneva, Group of Applied Physics, 20,Rue de l'Ecole de Médecine, CH-1211 Geneva 4, Switzerland*

*email: wolfgang.tittel@physics.unige.ch*

(November 4, 2018)

Long-distance Bell-type experiments are presented. The different experimental challenges and their solutions in order to maintain the strong quantum correlations between energy-time entangled photons over more than 10 km are reported and the results analyzed from the point of view of tests of fundamental physics as well as from the more applied side of quantum communication, specially quantum key distribution. Tests using more than one analyzer on each side are also presented.

PACS Nos. 3.65BZ, 3.67.Dd 42.81.-i

## I. INTRODUCTION

Entanglement, the possibility for a quantum system composed of several particles to be in a definite state while each single particle is in a mixed state, is one of the most interesting and puzzling predictions of quantum mechanics. The history goes back to 1935. Starting from the perfect 2-particle correlations predicted for entangled states, Einstein, Podolsky and Rosen argued that quantum theory is not complete [1]. In 1964, Bell demonstrated that the attempt to complete the theory with so called hidden variables and maintaining the locality condition leads to statistical predictions for measurements along nonorthogonal bases which differ from those given by standard quantum theory [2]. Tests of the so called Bell inequalities have been made again and again [3–7] in order to show more and more clearly that the quantum-correlations can not be explained by local hidden variables theories (LHVT). Today, most physicists are convinced that a future loophole-free test [8] will definitely demonstrate that nature is indeed nonlocal.

However, there is still interest in new experiments, the motivation is threefold. A first aim in future tests is to close the remaining loopholes. For instance, the fact that the detected pairs of particles form only a small and possibly biased subensemble of the created pairs, the so-called detection loophole [9], is under investigation at groups in Los Alamos [10], Texas [11] and Paris [12]. The locality loophole, based on the assumption that the properties of the correlated particles might be predetermined by the settings of the analyzers [13], has been examined by Aspect et al in 1982 [5]. Yet, the fast changing of the settings in order to prevent any influence on the photon pairs within the frame of special relativity has been criticized as not being really random [14]. Recently an experiment has been realized in Innsbruck in order to close remaining doubts on the locality loophole [15]. Our results with more than one analyzer on each side can also be considered in this context (see section V.A).

A second motivation for Bell-type tests is evolving from a recent proposal to use entangled particles for a test of relativistic nonlocality (or multisimultaneity), an alternative quantum theoretical description of nature which unifies nonlocality and relativity of simultaneity [16]. Such a test requires a large spatial separation between the different parts of the experiment. Hence it requires that the quantum correlations are maintained even when separating the particle over scales larger than the usual laboratory ones.

Third, besides these roles as candidates for tests of fundamental physics, entangled particles lie at the heart of the new field of quantum information processing (or quantum communication) which has evolved in rather big steps during the last years [17]. Its characteristics is to turn quantum conundrums into potentially useful processes which can not be achieved using classical physics. One of the most promising results of this new field is quantum key distribution [17,18], often also referred to as quantum cryptography, a way to establish a secret key between two parties which can be used afterwards to code and decode a message. The quantum mechanical law that a measurement of an unknown system will in most of the cases disturb the system is exploited here to reveal an eavesdropper: if none of the transmitted bits, coded in nonorthogonal states, have been disturbed, no unlegitimate third person has tried to listen in. Other examples for quantum information processing are dense coding [19] (the possibility to send more than one bit of classical information encoded in a single quantum bit) and teleportation [20] (transmission of an arbitrary quantum state from one particle to another one). Algorithms to factorize large numbers with a quantum computer are known and are much faster than those, known for classical computers [21]. The key word of the whole field of quantum information processing is entanglement. Two particle entanglement is required for dense-coding and teleportation and for some schemes of cryptography [22], entanglement of thousands of particles is needed for quantum computers. Hence the whole field relies on the existence of quantum nonlocality and on the fact that environment-induced decoherence [23] (and spontaneous collapses [24,25], if it exists) can be kept small or can be prevented for a sufficiently long time or distance.

In 1997 and 1998, we performed two series of experiments in order to examine whether energy-time entanglement is robust enough to be really exploited for the motivations mentioned in the last two paragraphs [26]. The aim of this article is to draw a concluding line under these Bell-type tests of quantum correlations over more than 10 kilometers, and to provide the reader with more information about experimental requirements than has been published in short letters [27,7]. As the results from the 1997 experiment [27] are confirmed in the 1998 one [7], we will mostly focus on the latter experiment as it is altogether more complex and uses more advanced technology. However, interesting experimental solutions, chosen in the 1997 experiment will be mentioned as well.

The outline of this paper is the following: After this introduction we will briefly present the theoretical background, for tests of Bell inequalities as well as for quantum cryptography (section II). Then, we will describe the experimental setup in section III. This part is divided into several sub-sections, each one focussing on a special detail: two-photon source, interferometers, dispersion in optical fibers, photon detectors, transmission of results of measurements, and measurement of correlations. Next, section IV, reports on the results. In addition to Bell tests implying one analyzer for each of the correlated particles, results for an experiment with three analyzers, two on one end and the third at the other end (10 km away) will be presented. Finally we will report on new data obtained in a laboratory (short distance) experiment using four analyzers, two on each side of the source. In the latter experiments, the two nearby devices analyse the incoming photons randomly, the choice being made by a passive beam splitter. These setups enable to test directly the CHSH form of Bell-inequalities [28]. Besides that, they can be seen in terms of closing the locality loophole. Beyond examining fundamental questions, our experiments establish also the feasibility of quantum cryptography with photon pairs as proposed by Ekert [22] over a significant distance. Two short paragraphs will briefly discuss our experiments from these two points of view (section V). Finally, a brief conclusion is given in section VI.

## II. THEORETICAL BACKGROUND

### A. Tests of Bell inequalities

A Bell-type experiment consists of the following parts: A source emitting pairs of correlated particles, propagating in different directions. Each particle enters an apparatus analyzing the correlated feature and ascribing a binary value ( $\pm 1$ ) to the outcome. The operation of each device is controlled by a knob which sets the parameters  $\delta_1$  ( $\delta_2$ ), e.g. phase shifts of interferometers (when dealing with energy-time correlations) or orientation of polarizers (when using polarization correlations). The classical information about the detection of a particle, namely when and where it is detected, is then sent to a coincidence electronic which measures the number of time-correlated events  $R_{i,j}(\delta_1, \delta_2)$ , ( $i, j = \pm 1$ ).  $R_{+-}$  denotes e.g. the coincidence count rate between the + labeled detector at apparatus 1 and the - labeled one at apparatus 2. This enables to calculate the so called correlation coefficient [4]

$$E(\delta_1, \delta_2) := \frac{R_{++}(\delta_1, \delta_2) - R_{+-}(\delta_1, \delta_2) - R_{-+}(\delta_1, \delta_2) + R_{--}(\delta_1, \delta_2)}{R_{++}(\delta_1, \delta_2) + R_{+-}(\delta_1, \delta_2) + R_{-+}(\delta_1, \delta_2) + R_{--}(\delta_1, \delta_2)} \quad (1)$$

To evaluate this coefficient from measured data, we have to assume that the actually detected particle pairs form a representative sample of all created pairs. The famous Bell-inequalities point out an upper limit for a combination of four such correlation coefficients with different analyzer settings  $\delta_1, \delta_2$  under assumption of local hidden variable theories (LHVT). One of the most often used form, known as the Clauser-Horne-Shimony-Holt (CHSH) Bell-inequality [28] is

$$S = |E(d_1, d_2) + E(d_1, d'_2) + E(d'_1, d_2) - E(d'_1, d'_2)| \leq 2, \quad (2)$$

where  $d_i, d'_i$  ( $i = 1, 2$ ) denote values of phases  $\delta_i$ .

We now describe the quantum mechanical predictions for a test of Bell-inequalities using energy-time entangled photons as proposed by Franson in 1989 [29]. Each one of the two entangled photons is directed into an unbalanced interferometer. Since the path-length difference of the interferometers, exactly the same for both of them, is much greater than the coherence length of the single photons, no single photon interference can be observed. With reference to experiments using polarization entangled photons, we refer to this as rotational invariance [30]. However, since two of the four processes leading to a coincidence detection (each photon can choose either the short or the long arm of the interferometers) are indistinguishable, fringes can be observed in the rate of coincidence detections between two detectors belonging to different interferometers. Due to the two noninterfering possibilities (the photons choose different arms) the visibility of the interference fringes is limited to 50%. However, the latter events can be excluded from registration provided the detection-time jitter is smaller than the time difference between passing through the

long or the short arm. The coincidences can then be resolved into two satellite peaks showing no interference effects and a central interference peak (see Fig. 2). Confining counting only to events in the middle peak [31], an entangled state is created where either both photons pass through the short arms or both through the long arms:

$$|\psi\rangle = \frac{1}{\sqrt{2}}\left(|s\rangle_1|s\rangle_2 + |l\rangle_1|l\rangle_2\right). \quad (3)$$

The two processes remain coherent with each other if the coherence length of the pump laser is longer than the difference between short and long arms of the interferometers. The maximum visibility can be increased in principle up to 100%. The quantum mechanical description leads via the coincidence function

$$R_{i,j}^{QM}(\delta_1, \delta_2) = m(1 + ijV \cos(\delta_1 + \delta_2)) \quad (4)$$

( $m$  being the mean value and  $i,j = \pm 1$ ) to the correlation function

$$E^{QM}(\delta_1, \delta_2) = V \cos(\delta_1 + \delta_2). \quad (5)$$

$V$  denotes the visibility, describing experimental deviation from the maximum value  $V=1$ . Using Eq. 5, the settings

$$d_1 = -\pi/4, d'_1 = \pi/4, d_2 = 0, d'_2 = \pi/2, \quad (6)$$

and assuming  $V = 1$ , Eq. (2) yields

$$S = 2\sqrt{2}. \quad (7)$$

This value is higher than the one predicted by LHVT. The violation thus shows that the description of nature as provided by quantum mechanics is unreconcilable with the assumptions leading to Bell-inequalities.

Another type of Bell-inequality was given by Clauser and Horne [30] for an experiment with polarizers. A similar argument can be applied to experiments using interferometers: if it is found experimentally that the single count rates are constant, and that  $E(\delta_1, \delta_2) = E(\Delta)$  holds where  $\Delta = |\delta_1 + \delta_2|$  is the sum of the phases in both interferometers, then Eq. 2 reduces to

$$S = |3E(\Delta) - E(3\Delta)| \leq 2 \quad (8)$$

Beyond that, if it is found that the correlation coefficient  $E$  is described by a sinusoidal function of the form (5), then Eq. 2 reduces to

$$S = \frac{4}{\sqrt{2}}V \leq 2. \quad (9)$$

Hence, observing a visibility  $V$  greater than

$$V \geq \frac{1}{\sqrt{2}} \approx 0.71 \quad (10)$$

will directly show that the correlations under test can not be explained by LHVT.

## B. Quantum key distribution

As pointed out by Ekert in 1991 [22], two-particle entanglement can be exploited for quantum key distribution. The same correlations used to show that nature can not be explained by LHVT can be used to establish a sequence of correlated bits between two users, usually called Alice and Bob. Moreover, a calculation of the Bell parameter  $S$  permits them to check whether a third, illegitimate party (usually called Eve) tried to extract information from the quantum channel. In 1992, two further protocols, similar to the so-called BB84 or 4-states protocol [32] and B92 or 2-states protocol [33], resp., but based also on quantum correlation of photon pairs have been published [34,35]. The setups are similar to the one already described to test Bell inequalities. We will describe only the latter proposal [35]. A source emits pairs of entangled particles flying back to back towards Alice and Bob. Both have an interferometer to their disposal. (We restrain ourself to energy time entangled photons but every kind of two particle entanglement will do as well.) For each incoming photon, Alice randomly choses phases of either  $d_A=0$  or  $d'_A=\pi/2$ , Bob randomly

applies either  $d_B=0$  or  $d'_B=-\pi/2$ . After a series of EPR particles has been measured, they announce publicly the settings of their analyzers but not which detector registered the photon. They then discard all measurements in which  $\delta_A + \delta_B \neq 0$  as well as the instances where either or both of them failed to register the photon. For the remaining instances ( $\delta_A + \delta_B = 0$ ) the results of their measurements should be perfectly correlated. To assess the security of their communication,

Alice and Bob publicly compare a random part of their key. If they find that the tested bits are perfectly correlated, they can infer that the remaining bits are also perfectly correlated and that no eavesdropper has tried to listen in. The remaining bits can now be used to form the cryptographic key.

In practice, also if no eavesdropper disturbed the key exchange, there will always be some corrupted bits due to imperfections of the experimental setup. Using standard error correction schemes, they can be localized and removed. However, since Alice and Bob can never be sure whether the presence of uncorrelated bits are due to the poor performance of their setup, they always have to assume that all errors are caused by an unlegitimized third person. The information about the key that Eve might have gained can be reduced arbitrarily close to zero using a procedure called privacy amplification [36]. However, this procedure only works if the common information between Alice and Bob is higher than the one between Eve and any of the two others. This is the case whenever the bits, Alice and Bob share, remain sufficiently well correlated in order to violate Bell inequalities [37].

It is interesting to note that besides ensuring the security of entanglement based quantum cryptography, the Bell inequality is even connected to the one qubit application of quantum cryptography: an eavesdropper (Eve) on a quantum channel can get more information than the receiver (Bob) if and only if the noise she necessarily introduces in the channel by eavesdropping is so large that Bell inequality can no longer be violated [37].

### III. EXPERIMENTAL SETUP

#### A. General setup

The schematic setup of the experiment is given in Fig. 1. A source creating pairs of energy-time entangled photons is placed at a telecommunication station near Geneva downtown. One of the correlated photons travels through 8.1 km of installed standard telecom fiber to an analyzer that is located in a second station in Bellevue, a little village 4.5 km north of Geneva. Using another installed fiber of 9.3 km, we send the other photon to a second analyzer, situated in a third station in Bernex, another little village 7.3 km southwest of Geneva and 10.9 km from Bellevue. Absorption in the connecting fibers are 5.6 dB and 4.9 dB, respectively, leading to overall losses in coincidences of about a factor of 10. The analyzers consist of all fiber-optical interferometers with equal path length differences. Behind the interferometers, the photons are detected by photon counters and the (now classical) signals are transmitted back to the source where the coincidence electronics is located. Finally, the results of the measurements made at different analyzers are compared in order to reveal the nonlocal correlations.

#### B. The two-photon source

The main elements forming a two-photon source are a pump laser and a nonlinear crystal (see also Fig. 1). To generate pairs of energy-time entangled photons suitable for long fiber transmissions, the pump laser has to have the following properties: Its wavelength must be adjustable in order to create photon pairs at a wavelength at which losses and pulse broadening caused by chromatic dispersion (see section dispersion in fibers) are small. In order to work in the second telecommunications window at 1310 nm, the wavelength of the pump laser (half the wavelength of the created photon pairs) should thus be tunable around 655 nm. Besides that, its coherence length must be large compared to the path-length difference short-long of the interferometers in order to maintain the coherence of the processes  $|s\rangle_1|s\rangle_2$  and  $|l\rangle_1|l\rangle_2$ . Commercially available laser diodes more or less meet these requirements. Their wavelength can be slightly tuned by changing their temperature. For example, a drop of 5°C will go along with a decrease of wavelength of  $\approx 1$  nm. The coherence length of such diodes varies with temperature and laser current and can attain values of up to 50 cm. In our 1997 experiment, we used a laser diode from RLT (6515G; 8 mW at 655.7 nm). The coherence length was long enough to demonstrate the existence of the entangled state (Eq. 3). However, in order to use energy-time entangled pairs for applications like quantum key distribution, a better performance is necessary. The two-photon source used in our 1998 experiment was based on a laser diode with external cavity (Sacher Lasertechnik; 10 mW at 654.8 nm) having a coherence length of around 100 m.

The light from the pump laser passes through a dispersion prism P to separate out the residual infrared fluorescence light and is focused into a KNbO<sub>3</sub> crystal (Casix) (see Fig.1). The crystal is oriented to ensure degenerate collinear

type-I phase matching for signal and idler photons at 1310 nm (hence the downconverted photons are both polarized orthogonally with respect to the pump photon). Due to these phase-matching conditions, the single photons exhibit rather large bandwidths of about 70 nm full width at half maximum (FWHM). Behind the crystal, the pump light is separated out by a filter F (RG 1000) while the passing down-converted photons are focused (lens L) into one input port of a standard 3-dB fiber coupler. Therefore half of the pairs are split and exit the source by different output fibers. The whole source including stabilization of laser current and temperature is of small dimensions and hence can easily be used outside the laboratory (in 1997 a box of about  $40 \times 45 \times 15 \text{ cm}^3$ , in 1998 two boxes, each of about  $30 \times 40 \times 15 \text{ cm}^3$ ).

### C. The interferometers

The two analyzers consist of all-fiber optical Michelson interferometers made of standard 3 dB fiber couplers. In the 1997 experiment we used chemically deposited end mirrors, in the 1998 one so called Faraday mirrors FM to reflect the light. (For the advantages of the latter solution see the section about dispersion in optical fibers and ref. [38].) The optical path-length differences (20 cm of optical fiber or 1 ns time difference in the 1997 experiment, 24 cm of optical fiber or 1.2 ns time difference in the 1998 one) are within  $10 \mu\text{m}$  equal in all interferometers. To control and change them, the temperature of the devices can be maintained constant or can slowly be varied.

To build fiber optical interferometers with almost identical path-length differences, we proceeded along the following lines (we first give the description for the 1998 experiment): In a first step we set up two interferometers with roughly 8 mm difference of path-length difference (from now on called discrepancy). In a second step, we measured the exact value of this discrepancy. To do so, we connected the two interferometers together with a third bulk-optical interferometer in series and illuminated them with a LED. When scanning the bulk-optical interferometer, one can find interferences if the path-length difference in the bulk optical interferometer equals the discrepancy within interferometers one and two. By this means one can measure this discrepancy with a resolution of a few  $\mu\text{m}$ . Changing the path-length difference of one of the two interferometer by cutting off the additional length of fiber, we were able to build interferometers with equal (within  $10 \mu\text{m}$ ) path-length differences. As we use Faraday mirrors to reflect the light, hence can not cut off the end of a fiber, we had to chop a piece of fiber in the middle of the arm. The tool used to cut the fiber precisely was made out of a fiber cleaver (Fujitsu) and a micro-translation stage. In the 1997 experiment, we directly cut the interferometers to have the most similar path-length differences possible. After having measured the discrepancy, we did the final alignment by polishing one interferometer arm. Only after this procedure the fiber ends were reflection coated.

In order to have access to the second output ports of the analyzers, normally coinciding with the input arm for Michelson interferometers, we used 3-port optical circulators C (JDS Fitel) in the 1998 experiment. This non-reciprocal device, based on the Faraday effect, enables to direct light from an input port 1 to output 2 and from port 2, serving now as input, to a third port regardless of the polarization state of the light.

### D. Dispersion in optical fibers

Two problems which have to be faced when using optical fibers are chromatic dispersion (CD) and polarization mode dispersion (PMD), especially when working with light of large bandwidth (in our case around 70 nm FWHM). For both effects, we have to distinguish between dispersion in the fibers connecting the source to the analyzers, and dispersion in the fibers forming the short and the long arms of the interferometers. However, for a good performance, both effects have to be seen in connection. We will first discuss the effects of chromatic dispersion.

In general, a light pulse travelling in dispersive media becomes broadened. In our case of coincidence detection of two photons, the increasing detection time jitter lead to a loss of temporal correlation between the two photons forming a pair. The resulting less perfect discrimination of the satellite coincidence peaks (see Fig. 2) then causes a smaller visibility. This problem could be solved using interferometers with larger path-length differences. However, different pulse broadening in the intereferometer arms, increasing with increasing arm-length difference, leads to a smaller visibility as well. It has been shown [39–42] that each of both CD effects, inside and outside the interferometer, can be cancelled out using photon pairs created by parametric downconversion. The strict anti-correlation of signal and idler photon enables to achieve a dispersion for one photon which is equal in magnitude but opposite in sign to that of the sister photon. The effect of broadening of the two wave packets then exactly wipes out (assuming a linear dependence of CD in function of the optical frequency, a realistic assumption). Two incidentally coincident photons stay coincident and no decrease of visibility due to different wave-packet broadening occurs. However this cancellation requires a choice of the frequencies of signal and idler photon which is determined by the dispersion properties of the

used fibers. As the fibers connecting source and interferometers and the fibers inside the interferometers are certainly not identical, complete cancellation of all dispersion effects at the same time is impossible. For instance, in the 1998 experiment we used a pump wavelength of 654.8 nm to create photon pairs at 1309.6 nm, leading to a dispersion caused time jitter which is below our limit of resolution, hence does not prevent from discriminating the satellite peaks. (The zero of CD for the fiber going to Bellevue is around 1312 nm, for the fiber going to Bernex around 1305 nm.) With two classical light pulses, this cancellation effect would be impossible. Even in the best case of centering the pulses around the zero of chromatic dispersion, we estimate a CD caused broadening of at least 600 ps for pulses of the same bandwidth. It is difficult to estimate the limitation of the visibility due to chromatic dispersion effects in the fibers forming the interferometers as we do not know the dispersion data of those fibers. However, even a deviation of a few nm from the zero dispersion wavelength (usually close to 1310 nm) causes only small effects. Therefore the influence on the visibility should be neglectable.

We now discuss the problems caused by PMD, first the effect of depolarization in the connecting fibers [43]. Indeed, if the relative delay  $\Delta\tau$  between the two modes of polarization transmitted by an optical fiber is larger than the coherence time of the photons (please note that the so called single mode fiber actually guides two modes of polarization), then an initially polarized photon completely loses its polarization. The single photons transmitted in our experiment have a bandwidth of approximately 70 nm (FWHM), corresponding to a coherence time  $\tau_c$  of around 90 fsec ( $FW\frac{1}{e}Max$ ). Using the standard value for PMD for modern telecommunication fibers of  $0.5 \text{ ps}/\sqrt{km}$ , and a fiber length of 8 km, we find  $\Delta\tau = 0.5 \frac{ps}{\sqrt{km}} \sqrt{8km} \approx 1.4 \text{ ps}$  which is more than one order of magnitude larger than  $\tau_c$ . Thus the photons arriving at the stations in Bellevue and Bernex, respectively, are completely depolarized, a result we confirmed in a separate experiment. Hence, an experiment using polarization entangled photons with similar bandwidth would be impossible. However, as our experiment does not take advantage of polarization entanglement, the effect of PMD in the connecting fibers is without consequences. In contrast to that, PMD in the fibers forming the interferometers either has to be avoided or to be compensated as it will lead to a decrease of visibility. In the 1997 experiment, we aimed to avoid all birefringence by placing the fibers which form the arms of the interferometer straight and without stress into copper tubes. However, a small temperature dependent birefringence could still be observed, probably caused by mechanical stress induced by the housing of the fiber coupler. To overcome this inconvenience, we used so called Faraday mirrors in the 1998 experiment [44]. This device consists of a  $45^\circ$  Faraday rotator in front of a conventional mirror to reflect the light at the end of the interferometer arms. These mirrors ensure that a photon, injected in any arbitrary polarization state into one of the interferometric arm will always come back exactly orthogonally polarized, regardless any birefringence effects in the fibers. Hence, no polarization alignment is required.

### E. The photon detectors

To detect the photons, we use germanium avalanche photodiodes (APD; NEC NDL5131P1) which we operate in the so called Geiger mode. This means that the bias voltage exceeds the breakdown voltage, leading an impinging photon to trigger an electron avalanche which then causes a macroscopic current pulse. After detection of this pulse, the avalanche has to be stopped and the diode to be charged again. A large (typically 50 k $\Omega$ ) resistor is connected in series with the APD. This causes a decrease of voltage across the APD below breakdown after the beginning of an avalanche, and thus leads to so called passive quenching of the avalanche. The recover time of the diode is given by the value of the quench resistor and their capacity. The emission of electrons trapped during the process of recharging leads to an elevated possibility to get a count not caused by a photon after an avalanche has taken place. The afterpulse fraction describes the probability to count such an afterpulse. For a more thorough review of photon counting with APDs, which is beyond the scope of this paper, we refer the interested reader to [45].

Unfortunately, germanium APDs show a lot of dark counts D, a higher afterpulse fraction and a smaller efficiency  $\eta$  compared to silicon APDs which can be used to count photons only of up to about 1000 nm wavelength. Hence, the advantage to use a wavelength where fiber losses are low in order to achieve long transmission distances has a drawback: the possibility to have an accidental coincidence caused by two dark counts happening at the same time or by a detection of a photon simultaneously with a dark count instead of the correlated photon which has been absorbed is high compared to short distance experiments using silicon detectors. Thus, the true coincidences might be hidden behind accidentals. The maximum achievable visibility for photon pair interference without subtraction of accidental coincidences is limited by the number of detected coincidences in the interference maximum (C) and the number of accidental ones (A).

$$V_{max} = \frac{C - A}{C + A}. \quad (11)$$

Hence, to achieve a visibility above 0.71, the ratio of detected to accidental coincidences (C/A) has to be larger than

$$C/A_{critic} = 5.9, \quad (12)$$

assuming no reduction of visibility due to any other causes.

As usual, we operate the APDs at liquid nitrogen temperature (77K) in order to decrease the number of dark counts. To quench the avalanches we use a relatively high resistor of 180 k $\Omega$ . The long recover time guarantees that most of the trapping centers are already empty before the diode is charged again, hence ensures a low afterpulse fraction. At the same time, the quantum-efficiency-to-noise ratio  $\eta/D$  increases. Besides the high quench resistor, in the 1998 experiment we implement large electronic deadtimes of about 4  $\mu$ s. By this means we suppress the counting of pulses when the diode is not completely charged, which would lead to an increasing time-jitter. In the 1997 experiment, a quench resistor of only 50 k $\Omega$  had been chosen and no extra electronic deadtime was applied. However, the performance of the subsequent time to pulse height converter (see section V.G.) ensures a similar deadtime, at least for the detector providing the start pulse.

To ensure that the overall quantum efficiencies in both detectors attached to the same interferometer are equal, we adjusted bias voltage and additional losses for both detectors in a way, that dark and light count rates are as similar as possible. We operated the detectors within a regime where dark count rates are of roughly 25 kHz, and we find quantum efficiencies of about 5%. The setup of our two-photon source leads to a separation of 50 % of the created photon pairs. Losses in the connecting fibers are 90 % and excess losses in each interferometer around 50%. In addition, we lose 50 % of coincidences due to a small coincidence window. Finally, and being a fundamental problem for Franson type experiments, the discrimination of the satellite coincidence peaks further reduces the coincidences by a factor of two. All together, we find a probability to detect an emitted photon pair of about  $8 \cdot 10^{-6}$ . The time jitter for the coincidence detection is around 350 ps FWHM and ensures a negligible contribution of the satellite coincidence peaks. We measure a ratio  $C/A$  of around 20 which permits to violate Bell inequalities without subtraction of accidental coincidences. Using the diodes at lower dark count rates would increase the fraction  $\eta/D$  even more, however, the growing time jitter would require a larger coincidence window, hence would lower the ratio  $C/A$ . Moreover a more important part of the satellite peaks would fall into the window as well.

## F. Transmission of results of measurements

The classical information about detection time and detector number has to be transmitted to a common place (in our case the place where the source is located). To do so, we use supplementary telecommunication fibers. The two possibilities to detect the photon (either detector + or -) is encoded in series of two short laser pulses separated by a short (detector -) or a long (detector +) delay. The pulses are detected by ordinary pin photodiodes and the delay between the pulses is transformed into the detector label again. Another possibility for transmission of the classical information would be to use one fiber for each detector. However the latter solution would bring up the need for additional pulsed lasers and pin photodiodes.

Care must be taken not to introduce additional time jitter during the processes of coding, transmission and decoding, as a large incertitude on the arrival time will lead to a loss of temporal coherence and hence to a superposition of the satellite and the central coincidence peaks.

## G. Measurement of correlations

In order to reveal the nonlocal correlations, one has to compare the results of the measurements at the distant analyzers. The signals from the pin photodiodes trigger time to pulse height converters (TPHC; Tenelec ?). We choose the signals coming from Bellevue to start, the signals coming from Bernex to stop the TPHCs. For each pairing of detectors belonging to different interferometers, we get a series of three peaks in the time spectrum (Fig 2). Window discriminators permit to count coincidences within intervals of a few hundred ps which are centered around the interference peaks. We measure the four different coincidence count rates  $R_{i,j}$  in a single run, yielding directly the correlation coefficient  $E(\delta_1, \delta_2)$  (Eq. 1) (in the 1997 experiment, only one coincidence function was measured, hence the correlation function had to be deduced from symmetry arguments).

Please note that it is important to register each pairing of detectors with a different TPHC. Indeed, separating coincidence peaks belonging to different couples of detectors only by introducing different delays between start and stop leads to summation of the accidental coincidences of all pairings and thus to a decrease of the ratio  $C/A$ . As we used only two TPHC, we utilized a kind of multiplexing in order to register all coincidence count rates. Each TPHC was triggered by two different pairings of detectors. By assigning each TPHC output to the belonging pairing, we could overcome the problem of counting the ensemble of accidental coincidences in each channel.

## IV. RESULTS

We monitored the four coincidence count rates as a function of time and slowly changed the phases  $\delta_1, \delta_2$  while measuring. As the coherence length of the single photons is five orders of magnitude smaller than the arm-length difference of the interferometers, no phase dependent variation of the single count rates can be observed. Hence our assumption of rotational invariance is well satisfied. However, the coincidence count rates as well as the correlation coefficient, calculated from the four rates using Eq. 1, show sinusoidal variation when changing the phases in the interferometers.

### A. Experiments with two interferometers

In order to test the quantum mechanical predictions that the correlation function depends only on the sum of the phases in both interferometers and not on the actual phases in either one, we perform the following experiment. We change the path-differences of both interferometers first in opposite directions, then in the same directions and compare the frequencies observed for the correlation function with the frequencies measured when scanning only one of the two interferometers (Fig. 3, table I, table II). Calculating the frequencies for a joint scan of both interferometers from the frequencies observed when scanning only one, we find them to be in almost perfect accordance with the measured values. From this, we can conclude that indeed the correlation function does depend on the sum of the phases in both interferometers ( $\delta_1 + \delta_2$ ) as described by Eq. 5. Hence we can calculate the parameter S from the observed visibilities (Eq. 9).

In all cases we systematically find values exceeding the limit given by the Bell-inequalities by at least 8 standard deviations ( $\sigma$ ). The raw data for a variation of the Bernex-interferometer yield a visibility of  $(86.2 \pm 1)\%$ , leading to  $S_{raw} = 2.44$  and a violation of Eq. 9 by  $15.5 \sigma$ . Most of the difference between this result and the theoretical prediction of  $S=2\sqrt{2} \approx 2.83$  can be attributed to accidental coincidences.

We measure them by delaying the stop signals by additional 8 ns. Therefore the signals representing correlated photons arrive apart from the detection window. We thus destruct all correlation between the signals from the two detectors, leaving only accidental coincidences to be measured. However, we find the true value if and only if there is no elevated coincidence rate caused by detection of a photon 8 ns before. Since the time spectrum shows an uniformly distributed noise floor (the detector deadtimes prevent from counting an afterpulse up to  $4 \mu s$  after detection of a photon), it is natural to assume that we can indeed infer from the measured to the true rate of accidental coincidences. Besides, the measured rate of  $26.4 \pm 1.3$  per 30 sec is in excellent agreement with the one we can calculate from the single count rates (39.5 kHz) and the size of the coincidence window ( $(550 \pm 10)$  ps). Indeed, by the latter means we find  $25.7 \pm 0.5$  accidental coincidences per 30 seconds. Subtracting them, we obtain  $V_{net} = (93.3 \pm 1.1)\%$ , corresponding to  $S_{net} = 2.64$  and a violation of Eq. 9 by  $20.5 \sigma$ .

In two further measurements we changed the path-length difference in either one of the two interferometers within a quite large range while the other interferometer is kept stable. The results are listed in table III. Fig. 4 shows the variation of the correlation coefficient observed for a scan in the Bellevue-interferometer. The correlation function shows a sinusoidal function with a gaussian envelope representing the coherence length of the single photons [46]. From this envelope, we calculate a coherence length of around  $13 \mu m$  corresponding to a bandwidth of around 70 nm FWHM. Fitting only the two central periodes of the correlation functions with a sinusoidal function, we find visibilities of up to  $V_{raw} = (85.3 \pm 0.9)\%$  ( $V_{net} = (95.5 \pm 1)\%$ ), leading to  $S_{raw} = 2.41$  ( $S_{net} = 2.70$ ) and a violation of Eq. 9 by  $16.2 \sigma$  ( $24.8 \sigma$ ).

Besides determining the correlation functions for the above mentioned measurements, we made fits of the underlying coincidence functions  $R_{i,j}$  ( $i,j=\pm 1$ ) as well. The results can be found in tables I and III. We find the visibilities to be in close agreement with the values for the correlation function. However, even if the single count rates show almost perfect symmetry, there is a difference in the mean values of the coincidence counts. We found the cause for this effect to be the large bandwidth of the single photons in connection with different spectral quantum efficiencies of the different detectors. Therefore the sum of the coincidence rates of one detector with both detectors on the other side (i.e.  $R_{++} + R_{+-}$ ) is not constant. However, if summing over all coincidence rates, we always find the same value, confirming that the size of the detected samples of photon pairs does not change.

### B. Experiments with three interferometers

In order to test the CHSH-Bell inequality (Eq. 2), we have to measure the correlation coefficients for the discrete phase differences given in Eq. 6. To do so, we modify our setup in the following way (see inlet in Fig. 1). The fiber



arriving in Bellevue is connected to a standard 3 dB fiber coupler. Each output arm of this coupler is followed by an interferometer of the same kind as described before. Hence each incoming photon is analyzed by one of the two different phase settings. As we did not have enough circulators and detectors, we were able to observe only one output of each analyzer. For this reason we could only measure two of the four coincidence count rates needed to calculate the correlation function (Eq. 1). To infer from the measured functions to the correlation function we thus have to assume the same symmetry between the coincidence functions as we found in the experiments described before. With this quite natural assumption, we can evaluate the correlation functions  $E(d_1, d_2)$  and  $E'(d'_1, d_2)$  at the same time, hence for exactly the same setting  $d_2$ . Fig. 5 shows the correlation coefficients observed when changing the phase  $\delta_2$  in the Bernex interferometer. We find again sinusoidal functions, the parameters for best fits are listed in table IV. For the difference of phases  $\delta_1 - \delta'_1$  between the two interferometers in Bellevue we obtain  $\pi/2.25$ , which is close to the ideal value of  $\pi/2$ , needed to maximally violate Bell inequalities. Visibilities are about 77.5% without and about 95.5% with subtraction of accidental coincidences. We can now directly evaluate the value of the Bell parameter S from looking at the correlation coefficients for two different parameters  $\delta_2$ . For the indicated points we find  $S_{raw} = 2.38 \pm 0.16$  and  $S_{net} = 2.92 \pm 0.18$  leading to a violation of 2.4 respectively 5.1 standard deviations. Using the parameters obtained for the best fits in order to more precisely determine value and incertitude of the four points, we find  $S_{raw} = 2.186 \pm 0.033$  and  $S_{net} = 2.692 \pm 0.038$  leading to a violation of 5.6 respectively 18.2 standard deviations.

### C. Experiments with four interferometers

In order to measure all four different correlation coefficients required to test the CHSH-Bell inequality at the same time, we perform an experiment with four interferometers, one couple on each side of the source. This time, the whole setup is located in our laboratory. The interferometers are placed 2 meters from the source with connecting fibers of 5 meters. Each combination of interferometers leads to a different correlation coefficient. Again we can measure only four different coincidence rates and thus have to assume the same symmetry as we already did before. Doing so, we can calculate the correlation coefficient by normalizing the coincidence rates with their mean value. From Eq. 4 and Eq. 5 we get

$$E_k(\delta_1, \delta_2) = \frac{R_k(\delta_1, \delta_2)}{m} - 1, \quad (13)$$

$k$  denoting one of the four possible combinations of interferometers. We fix the difference between phases of one couple of interferometer ( $I_3, I_4$ ) to be  $\pi/2$ . Then we scan the two other interferometers with different frequencies. This leads to sinusoidal variation of all coincidence rates (see Fig 6). Best fits enable to very precisely determine mean values, frequencies and phases (see table V). Using Eq. 13 we calculate the correlation coefficients  $E_k$ , leading to the Bell-parameters S

$$S = E_1 + E_2 + E_3 - E_4. \quad (14)$$

The results are shown in Fig 7. Using the values of the four indicated points, we find  $S_{raw} = 2.41$  ( $S_{net} = 2.63$ ) and a violation of the CHSH-Bell inequality by 5.1  $\sigma$  (7.5  $\sigma$ ). The theoretical prediction for a phase difference of  $\pi/2$ , sinusoidal functions and equal visibilities for all correlation functions leads to

$$S_{theo} = -2\sqrt{2}V \sin\left(\frac{t-a_1}{2\omega_1} + \frac{t-a_2}{2\omega_2}\right) \sin\left(\frac{t-a_1}{2\omega_1} - \frac{t-a_2}{2\omega_2} - \frac{\pi}{4}\right) \quad (15)$$

with  $t$  being the time in numbers of measurement intervals. Using frequencies and phases found by fitting the correlation coefficients (Fig 6, table V) and fitting only the visibility  $V$ , we find  $V_{raw} = (86.6 \pm 1.1)\%$ , ( $V_{net} = (94.2 \pm 1.1)\%$ ) leading to  $S_{raw} = 2.45$  ( $S_{net} = 2.66$ ) and a violation of the CHSH-Bell inequality by 14.5  $\sigma$  (22  $\sigma$ ) (see also table V).

## V. DISCUSSION

All our experimental results are in good agreement with quantum mechanics. The measured two photon fringe visibility around 86% can be almost entirely explained by the detectors noise. And since we found a similar netto visibility of  $(94.3 \pm 0.5)\%$  in an experiment carried out in our lab, one has to conclude that the distance does not affect the nonlocal aspect of quantum mechanics, at least not for distances up to 10 km. As already mentioned in the introduction, no experiment up to date could close the detection loophole. In particular, long-distance experiments

will probably never be suitable for a decisive test as transmission losses will always be too high to allow detection of more than 66.7% of the created photons [47]. Below we discuss separately the relevance of our results for the debate on the locality loophole and for applications in quantum cryptography.

### A. The locality loophole

The locality loophole is based on the assumption that, somehow, the settings  $\delta_1$  and  $\delta_2$  of the analyzers influence the photon pairs emitted by the source. Hence, each settings would analyze differently prepared photons. In order to close this loophole, the settings should be chosen only after the photons left the source. Hence, long distance experiments are favourable. Ideally, a physicist (or any being enjoying freedom) would make the setting's choice. But in practice, random number generators are used. In the experiment by Aspect et al. [5], a "periodic" random number generator determines into which of two analyzers with fixed parameter settings the particles are sent (for a discussion on its randomness see [14]). Obviously, our setups with three and with four interferometers are quite similar to the one chosen by Aspect, provided one assumes that the photon takes a random choice at the fiber coupler and that this choice is not predetermined by a hidden variable which "knows" the settings of the analyzers behind the coupler. Let us briefly elaborate on this point. A possible objection would be to refute the existence of randomness. But if randomness exists, a "quantum random number generator" would qualify as the best possible choice. Admittedly, one could argue that it would be preferable that this quantum choice is made by a system independent of the particle under test. This outside random number would trigger a fast electro-optic switch. In practice such switches (Lithium Niobate modulators) have losses higher than 50%, hence it would be equally practical to use a passive splitter, as in our experiment and to turn off the detectors of one of the analyzer! Turning off detectors can certainly not improve the experiment. But from a logical point of view, the above discussion shows that the locality loophole is not independent of the detection loophole, since for low detection efficiency passive splitters are equivalent to active ones.

### B. Quantum key distribution

Let us turn now to the first promising application of entangled particles in the field of quantum communication, quantum key distribution (QKD). The quantum bit error rate (QBER, the number of wrong bits divided by the number of transmitted bits) of this scheme is related to the visibility  $V$  of the coincidence function before removal of the accidental coincidences:  $\text{QBER} = \frac{1-V}{2}$ . Note, that subtracting the accidentals is impossible for quantum cryptography, as there is no way to determine which coincidence counts are accidental and which are due to a photon pair. To guarantee the security of the transmission, the visibility of the coincidence functions has to be above  $\frac{1}{\sqrt{2}}$ , hence the quantum bit error rate below  $\approx 15\%$ . Since we achieve raw visibilities of up to 85.2% from which we can infer to a QBER of 7.4%, we demonstrate that quantum key distribution with photon pairs is possible, even over distances of more than 10 kilometers.

Our source and analyzers are easy to transport and our setup does not depend on specially manufactured fibers but can be installed in every modern singlemode fiber network working at 1310 nm. Beyond that, it does not require active polarization control. Therefore it is very promising for practical implementation of QKD, not far from existing QKD schemes working with weak pulses [49]. However, a fast switching in order to really exchange a key still has to be implemented. This switching can be done either by a phase modulator or, as we did in our last experiments by using a fiber coupler connected to two interferometers with appropriate phase differences. The advantage of such a setup is that no fast random generator and switching electronic is necessary. However, as the visibility and hence the QBER decreases due to increasing losses, this setup is in our case limited to around 10 km, a distance which is determined by the number of created photon pairs, overall losses and detector performance. A better way to do entanglement-based quantum cryptography would be to use a source employing nondegenerate phasematching in order to create correlated photons of different wavelengths, one at 1310 nm, the other one around 900 nm. This would allow to use more efficient and less noisy silicon photon counting modules to detect the photons of the lower wavelength. To avoid the high transmission losses of photons of this wavelength in optical fibers, the interferometer(-s) measuring these photons could be placed next to the source. First investigations show that quantum cryptography over tens of kilometers should be possible.

## VI. CONCLUSION

In conclusion, we have reported on experiments demonstrating strong two-photon correlations over more than 10 kilometers. Provided that our results are not affected by the remaining loopholes, we thus can confirm that nature can not be described by LHVT. Beyond that, our experiments support the prediction of quantum mechanics that distance has no effect on these quantum correlations. The experimental difficulties and possible solutions have been discussed in length.

The feasibility of long-distance experiments now opens the door for several interesting possibilities, both in the field of fundamental tests of quantum physics, as in the field of emerging applications of quantum information processing. Among the latter, let us mention, in addition to quantum cryptography which is discussed in this article, the fascinating possibility of entanglement swapping [50], dense coding [19] and of quantum teleportation [20] at large distances. Among the even more fundamental issues, one interesting possibility is to test relativistic nonlocality [16]: Set one analyzer in motion such that each on analyzer in his own inertial frame detects his photon first. The projection postulate is then difficult to apply, if it applies at all [51].

## ACKNOWLEDGMENTS

This work was supported by the Swiss FNRS and Priority Program for Optics, by the European TMR network "The physics of Quantum Information", contr. no. ERBFM-RXCT960087, and by the Fondation Odier. We like to thank G. Ribordy and T. Herzog for help during the experiments as well as J. D. Gautier and O. Guinard for technical support. The access to the telecommunication network was provided by Swisscom and the circulators by JDS.

---

- [1] A. Einstein, B. Podolsky and N. Rosen, *Phys. Rev.* **47**, 777 (1935).
- [2] J. S. Bell, *Physics* **1**, 195 (1964).
- [3] J. Freedman, and J. F. Clauser, *Phys. Rev. Lett.* **28**, 938 (1972); A. Aspect, P. Grangier, and G. Roger, *Phys. Rev. Lett.* **47**, 460 (1981); Z. Y. Ou and L. Mandel, *Phys. Rev. Lett.* **61**, 50 (1988); P. G. Kwiat, K. Mattle, H. Weinfurter, A. Zeilinger, A. V. Sergienko, and Y. H. Shih, *Phys. Rev. Lett.* **75**, 4337 (1995). J. G. Rarity and P. R. Tapster, *Phys. Rev. Lett.* **64**, 2495 (1990); J. Brendel, E. Mohler, and W. Martienssen. *Europhys. Lett.* **20**, 575 (1992); D. V. Strekalov, T. B. Pittman, A. V. Sergienko, Y. H. Shih, and P. G. Kwiat, *Phys. Rev. A* **54**, R1 (1996).
- [4] A. Aspect, P. Grangier, and G. Roger, *Phys. Rev. Lett.* **49**, 91 (1982).
- [5] A. Aspect, J. Dalibard, and G. Roger, *Phys. Rev. Lett.* **49**, 1804 (1982).
- [6] P. R. Tapster, J. G. Rarity, and P. C. M. Owens, *Phys. Rev. Lett.* **73**, 1923 (1994).
- [7] W. Tittel, J. Brendel, H. Zbinden, and N. Gisin. Submitted to *Phys. Rev. Lett.*
- [8] All experiments up to now rely on some unproven assumptions, leaving loopholes for local hidden variables theories.
- [9] P. Pearle, *Phys. Rev. D* **2**, 1418 (1970); E. Santos, *Phys. Lett. A* **212**, 10 (1996).
- [10] P. Kwiat et al., *Phys. Rev. A* **49**, 3209 (1994).
- [11] E.S. Fry, T. Walther, and S. Li, *Phys. Rev. A* **52**, 4381 (1995).
- [12] Even if not explicitly mentioned, the following experiment has the potential to close the detection loophole: E. Hagley et al., *Phys. Rev. Lett.* **79**, 1 (1997).
- [13] E. Santos, *Phys. Lett. A* **200**, 1 (1995).
- [14] A. Zeilinger, *Phys. Lett. A* **118**, 1 (1986).
- [15] private communication. The experiment has been proposed in G. Weihs, H. Weinfurter, and A. Zeilinger, in *Experimental Metaphysics*, edited by R. S. Cohen et al. (Kluwer, Dordrecht, 1997), pp.239-246.
- [16] A. Suarez and V. Scarani, *Phys. Lett. A* **232**, 9 (1997).
- [17] Special issue on quantum communication, *Physics World*, March 1998.
- [18] C. H. Bennett, G. Brassard, and A. K. Ekert, *Scientific American*, October 1992.
- [19] C. H. Bennett and S. J. Wiesner, *Phys. Rev. Lett.* **69**, 2881 (1992); K. Mattle, H. Weinfurter, P. G. Kwiat, and A. Zeilinger. *Phys. Rev. Lett.* **76**, 4656 (1996).
- [20] C. H. Bennet et al., *Phys. Rev. Lett.* **70**, 1895 (1993); D. Bouwmeester et al., *Nature* **390**, 575 (1997). D. Boschi et al., *Phys. Rev. Lett.* **80**, 1121 (1998).
- [21] P. W. Shor, in *Proc. 35th Annual Symp. on Foundations of Computer Science*, Santa Fe, ed. S. Goldwasser, p.124 (IEEE Computer Society Press, Los Alamitos 1994).
- [22] A. K. Ekert, *Phys. Rev. Lett.* **67**, 661 (1991).
- [23] W. H. Zurek, *Phys. Today*, **44**(10), 36 (1991). For comments by several authors see *Phys. Today* **46**(4) (1993).
- [24] W. H. Furry, *Phys. Rev.* **49**, 393 (1936).
- [25] G.C. Ghirardi, A. Rimini and T. Weber, *Phys. Rev. D*, **34**, 470 (1986).
- [26] A first attempt to investigate nonlocality over large distances has been reported in [6]. However, it contrasts with ours as both analyzers were sitting next to the source, one connected with a 4.3 km fiber on a spool, while the other analyzer was directly connected to the source. Therefore the physical distance between the two analyzers was of only a few meters.
- [27] W. Tittel et al., *Phys. Rev. A* **57**, 3229 (1998).
- [28] J. F. Clauser, M. A. Horne, A. Shimony, and R. A. Holt, *Phys. Rev. Lett.* **23**, 880 (1969).
- [29] J. D. Franson, *Phys. Rev. Lett.* **62**, 2205 (1989).
- [30] J. F. Clauser, and M. A. Horne, *Phys. Rev. D* **10**, 526 (1974).
- [31] J. Brendel, E. Mohler, and W. Martienssen, *Phys. Rev. Lett.* **66**, 1142 (1991).
- [32] C. H. Bennett, and G. Brassard, in *Proceedings of IEEE International Conference on Computers, Systems, and Signal Processing*, Bangalore, India (IEEE, New York, 1984), p. 175.
- [33] C. H. Bennett, *Phys. Rev. Lett.* **68**, 3121 (1992).
- [34] C. H. Bennett, G. Brassard, and N. D. Mermin, *Phys. Rev. Lett.* **68**, 557 (1992).
- [35] A. K. Ekert, J. G. Rarity, P. R. Tapster, and G. M. Palma, *Phys. Rev. Lett.* **69**, 1293 (1992).
- [36] C. H. Bennett, F. Bessette, G. Brassard, L. Salvail, and J. Smolin, *J. Cryptology* **5**, 3 (1992).
- [37] N. Gisin and B. Huttner, *Phys. Lett. A* **228**, 13 (1997); Ch. Fuchs et al., *Phys. Rev. A* **56**, 1163 (1997). Actually, in these paper one assumes that the eavesdropper can only measure one qubit after the other (though see N. Gisin and I. Cirac, *Phys. Lett. A* **229**, 1 (1997) and H. Bechmann-Pasquinucci and N. Gisin, quant-ph 9807041).
- [38] W. Tittel, J. Brendel, T. Herzog, H. Zbinden, and N. Gisin, *Europhys. Lett.* **40**, 595 (1997).
- [39] J. D. Franson, *Phys. Rev. A* **45**, 3126 (1992).
- [40] A. M. Steinberg, P. G. Kwiat, and R. Y. Chiao, *Phys. Rev. Lett.* **68**, 2421 (1992). A. M. Steinberg, P. G. Kwiat, and R. Y. Chiao, *Phys. Rev. A* **45**, 6659 (1992).
- [41] T. S. Larchurk, M. V. Teich, and B. E. A. Saleh, *Phys. Rev. A* **52**, 4145 (1995).
- [42] J. Brendel, H. Zbinden, and N. Gisin, *Optics. Comm.* **151**, 35 (1998).
- [43] N. Gisin et al., *Pure Appl. Opt.* **4**, 511 (1995).
- [44] M. Martinelli, M. J. Marrone, and M. A. Davis, *J. Mod. Opt.* **39**, 451 (1992).
- [45] P. C. M. Owens, J. G. Rarity, P. R. Tapster, D. Knight, and P. D. Townsend, *Appl. Opt.* **33**, 6895 (1994). A. Lacaita, P.

- A. Francese, F. Zappa, and S. Cova, *Appl. Opt.* **33**, 6902 (1994).
- [46] Unequal path-length differences in both interferometers  $\delta_1 - \delta_2 \neq 0$  increase the possibility to differentiate between the long-long and short-short paths (by looking at the differences in photon arrival time), hence decrease the visibility.
- [47] P. H. Eberhard, *Phys. Rev. A* **47**, R747 (1993).
- [48] The necessity to change the settings of the analyzers during the flight of the particles has been pointed out for the first time by D. Bohm, and Y. Aharonov, *Phys. Rev.* **108**, 1070 (1957)
- [49] C. Marand, and P. Townsend, *Optics Lett.* **20**, 1695 (1995); R. Hughes, G. Luther, G. Morgan, G. Peterson, and C. Simmons, *Lecture Notes in Computer Science*, **1109**, 329 (1996); H. Zbinden, G. D. Gautier, N. Gisin, B. Huttner, A. Muller, and W. Tittel, *Electronics Lett.* **33**, 586 (1997).
- [50] C. H. Bennet et al, *Phys. Rev. Lett.* **70**, 1895 (1993); M. Zukowski et al., *Phys. Rev. Lett.* **71**, 4287 (1993); J.W. Pan et al., *Phys. Rev. Lett.* **80**, 3891 (1998).
- [51] Y. Aharonov, and D. Z. Albert, *Phys. Rev. D*, **24**, 359 (1981).

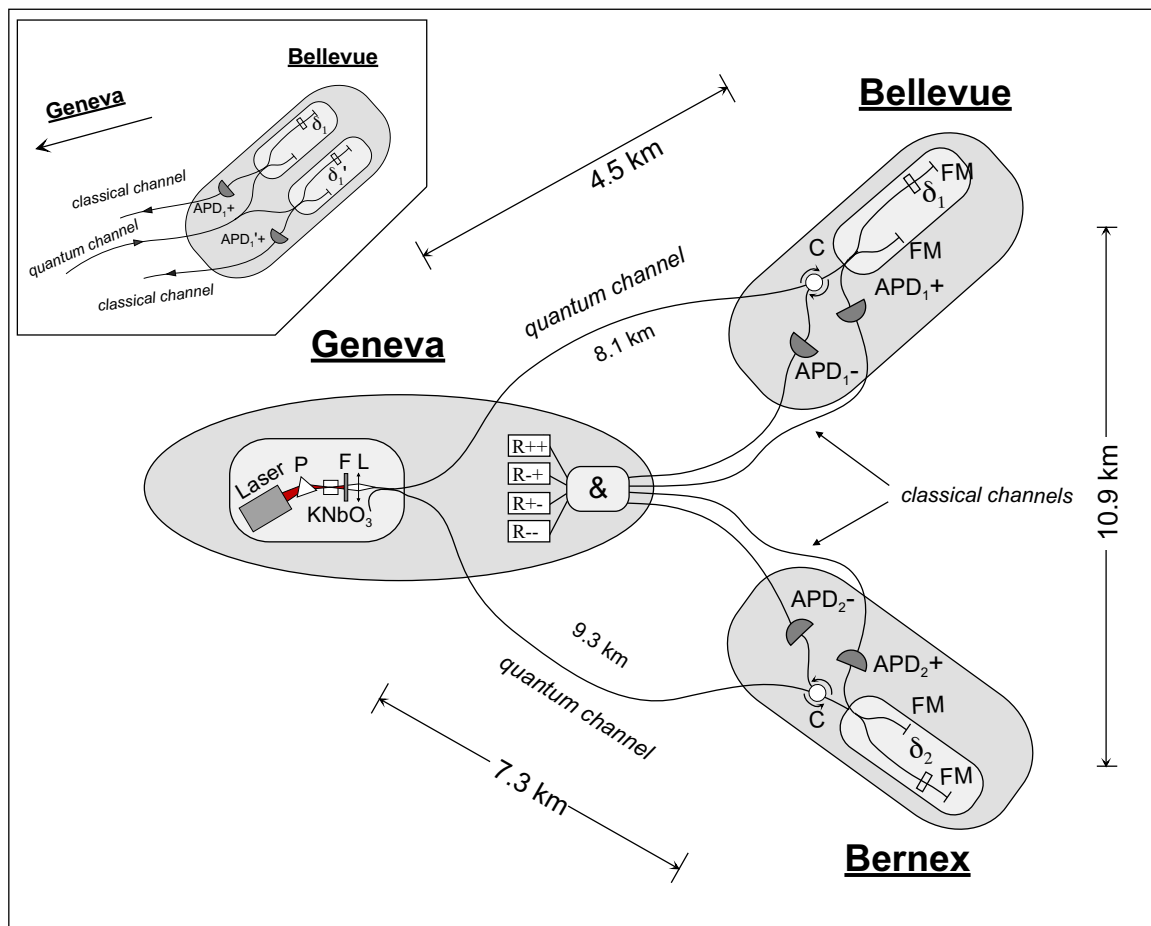


FIG. 1. Setup for experiments with two and three interferometers (inlet). See text for detailed description.

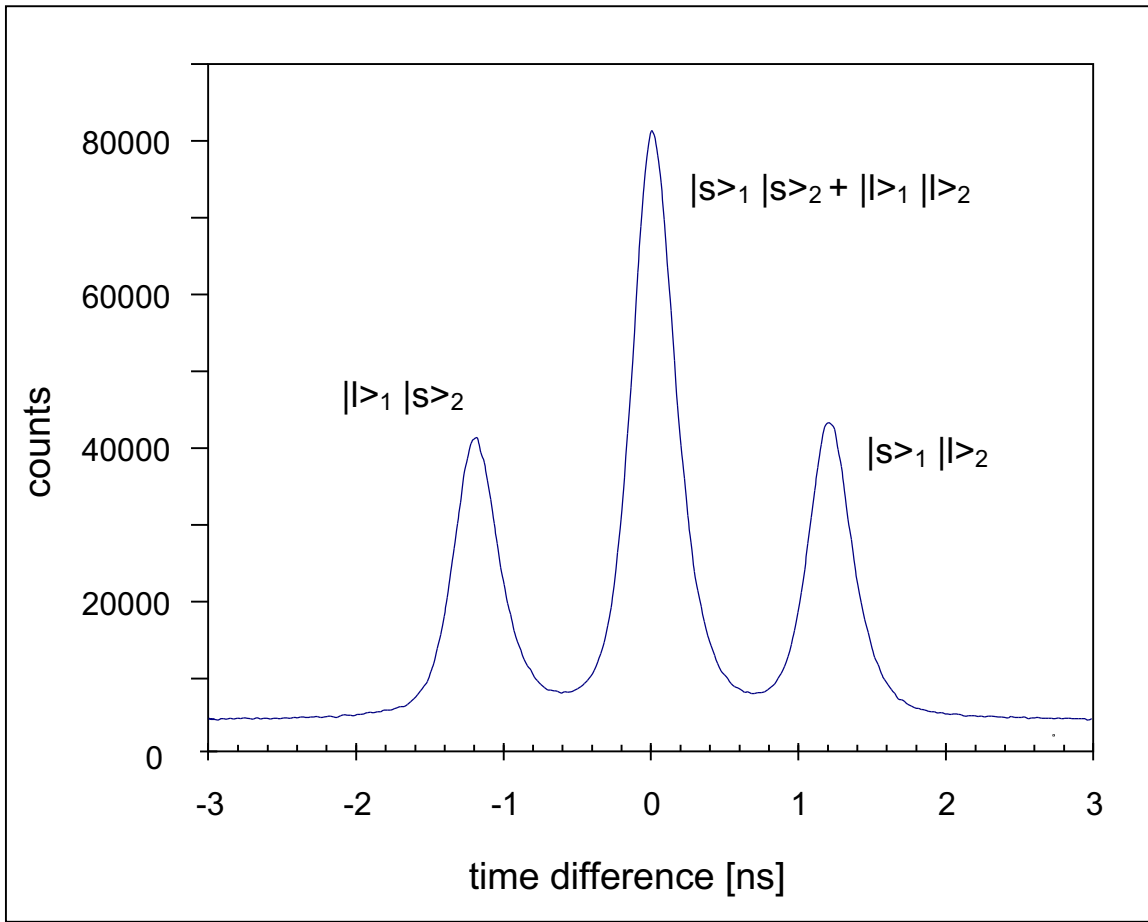


FIG. 2. Measured distribution of differences in arrival time of correlated photons. The satellite peaks belong to the transmission processes long-short (left hand side), and short-long (right hand side), respectively, in the interferometers. The two undistinguishable possibilities short-short and long-long lead to a detection within the central peak. Here shown is a noninterfering case. The width of the coincidence peaks is around 350 ps (FWHM).

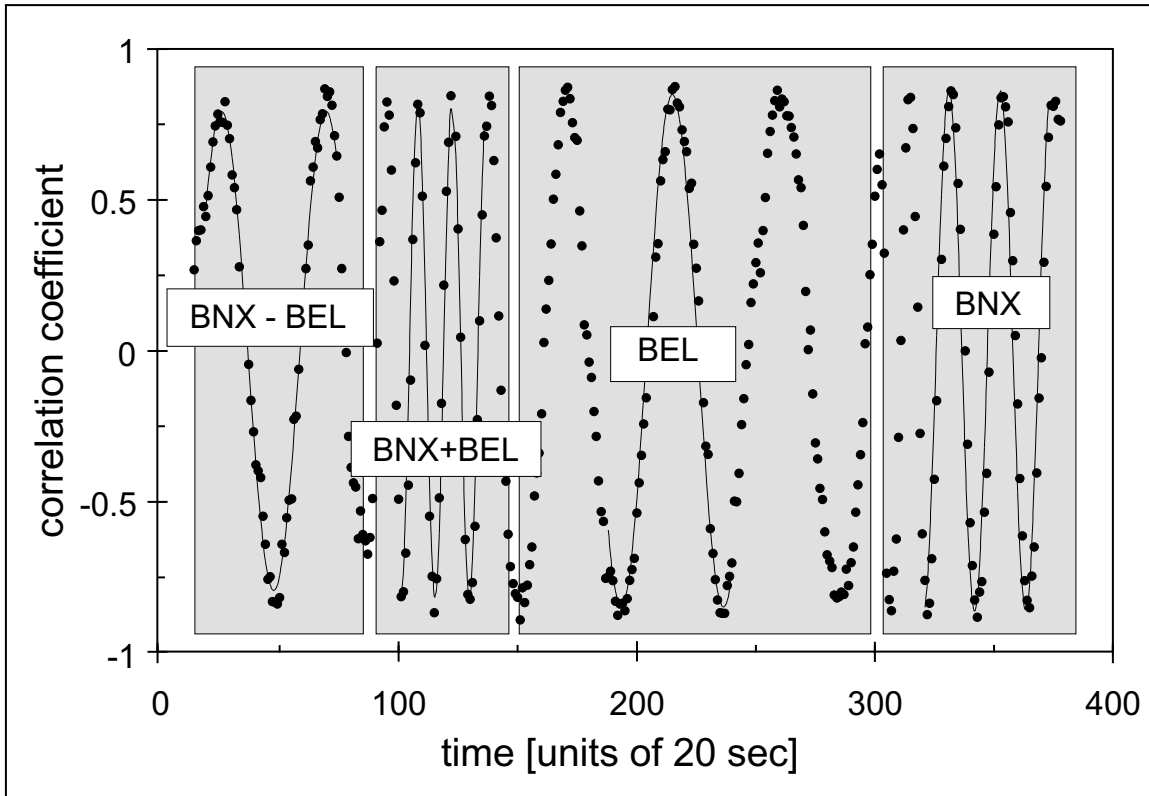


FIG. 3. Correlation coefficients observed while simultaneously changing the phases in both interferometers.

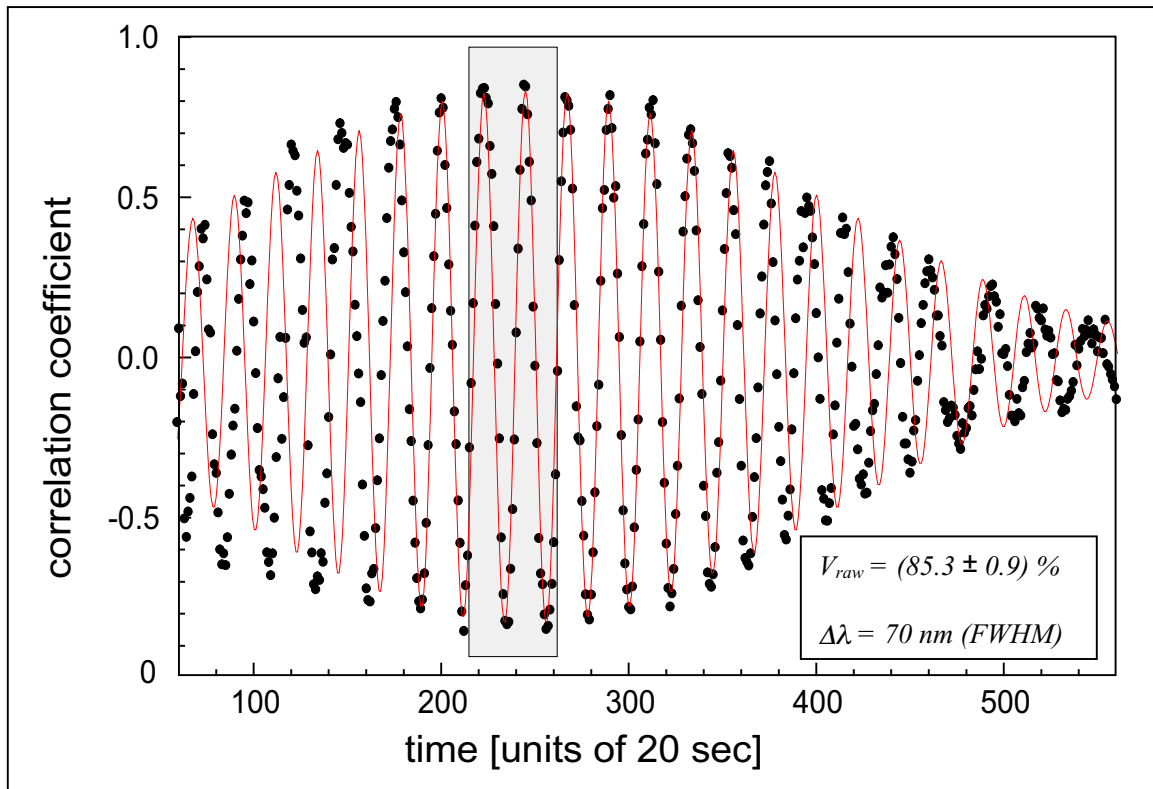


FIG. 4. Correlation coefficients measured for large phase-change in the Bellevue interferometer. The shaded region indicates the region for the fit over two periods.



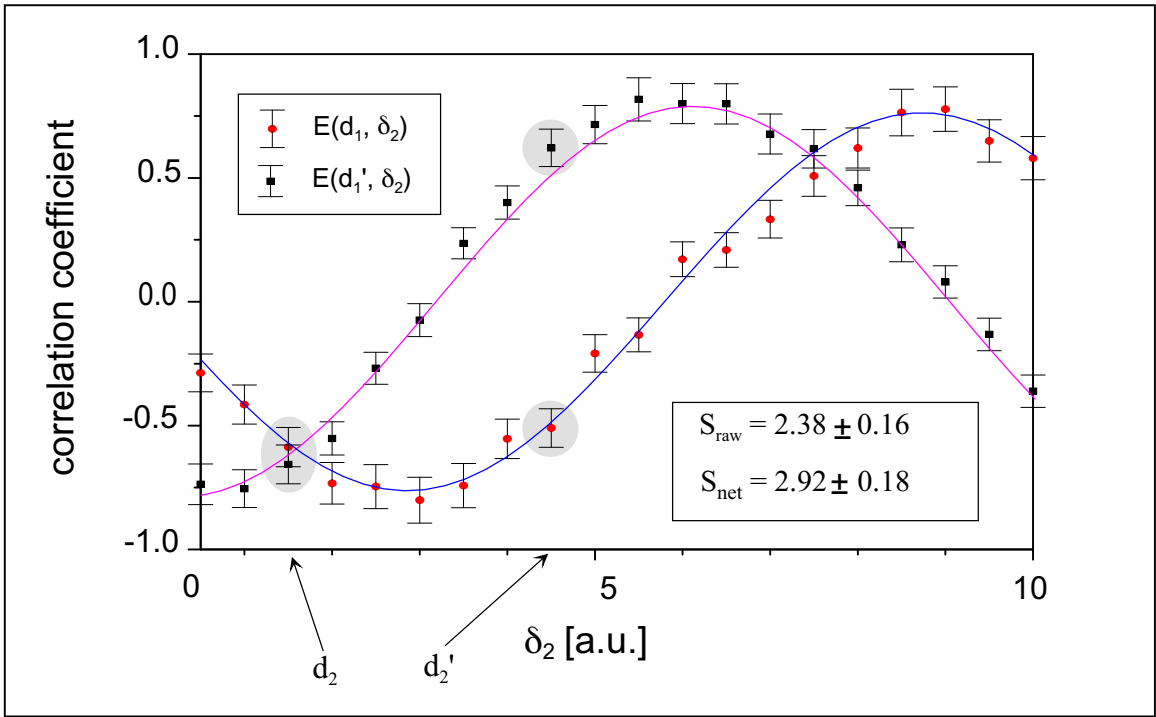


FIG. 5. Correlation coefficients observed in the experiment with three interferometers.

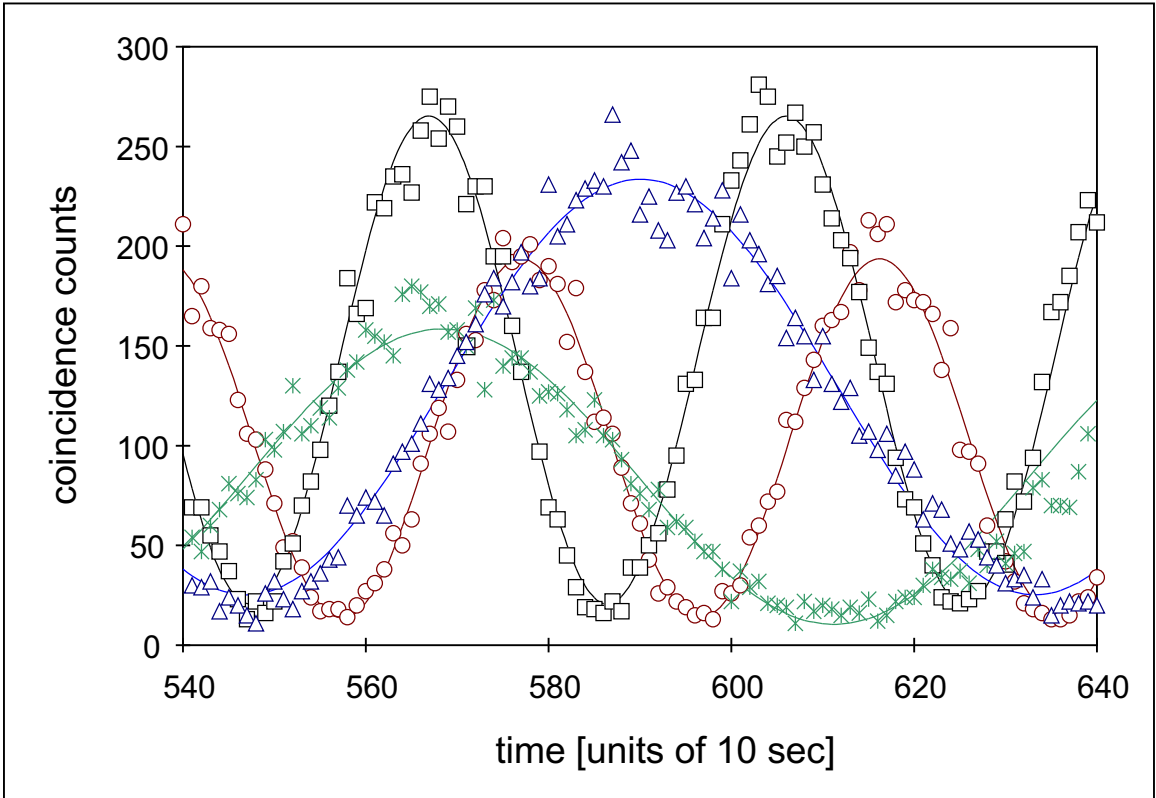


FIG. 6. Coincidence count rates observed in the experiment with four interferometers.

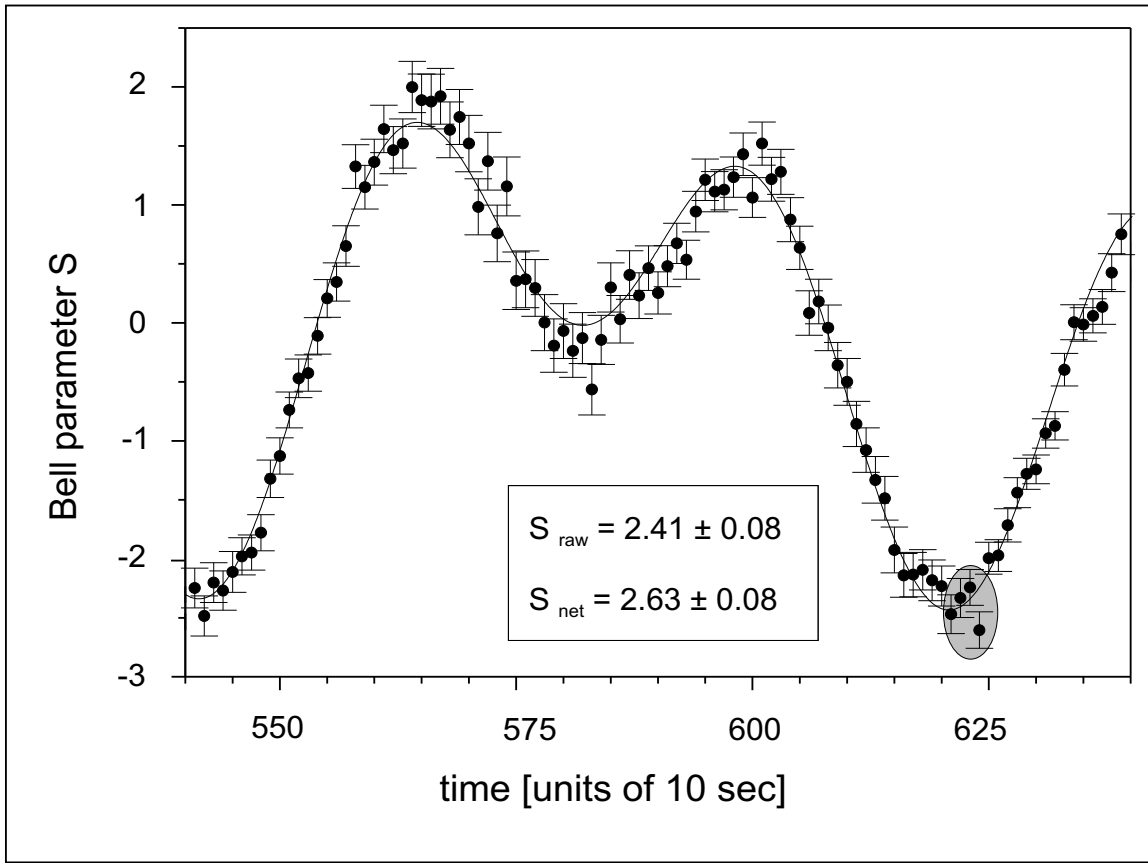


FIG. 7. Bell parameter  $S$  in the experiment with four interferometers.

Scan in			BNX		BEL		BNX-BEL		BNX+BEL	
			raw	netto	raw	netto	raw	netto	raw	netto
coincidence counts		accidental	mean value		mean value		mean value		mean value	
	$R_{++}$	$10.4 \pm 1$	$142.2 \pm 1.7$	$131.8 \pm 1.9$	$136.8 \pm 1.6$	$126.4 \pm 1.9$	$134.8 \pm 1.7$	$124.4 \pm 1.9$	$126.7 \pm 1.6$	$116.3 \pm 1.9$
	$R_{+-}$	$11.2 \pm 1.1$	$155 \pm 1.7$	$143.8 \pm 1.9$	$153.9 \pm 1.7$	$142.7 \pm 2$	$155.4 \pm 1.7$	$144.2 \pm 2$	$161.2 \pm 1.8$	$150 \pm 2.1$
	$R_{-+}$	$11.6 \pm 1.1$	$128.4 \pm 1.6$	$116.8 \pm 1.9$	$128.8 \pm 1.6$	$117.2 \pm 1.9$	$127 \pm 1.6$	$115.4 \pm 1.9$	$135.3 \pm 1.7$	$123.7 \pm 2$
	$R_{--}$	$10.7 \pm 1$	$140.7 \pm 1.7$	$130 \pm 1.9$	$137.4 \pm 1.7$	$126.71.9$	$150.6 \pm 1.7$	$139.9 \pm 2$	$135.5 \pm 1.7$	$124.8 \pm 1.9$
visibilities			coincidence functions		coincidence functions		coincidence functions		coincidence functions	
	$R_{++}$		$86.8 \pm 1.1$	$93.6 \pm 1.1$	$86.8 \pm 0.9$	$94 \pm 0.9$	$80.4 \pm 1.2$	$87.1 \pm 1.3$	$84.9 \pm 1.3$	$92.5 \pm 1.5$
	$R_{+-}$		$89.2 \pm 1.1$	$96.1 \pm 1.2$	$87.5 \pm 1.1$	$94.4 \pm 1.2$	$82.5 \pm 0.9$	$88.9 \pm 0.9$	$80.4 \pm 1.3$	$86.4 \pm 1.4$
	$R_{-+}$		$87.1 \pm 1.2$	$95.7 \pm 1.4$	$84.1 \pm 1.3$	$92.5 \pm 1.4$	$80.2 \pm 1$	$88.3 \pm 1.1$	$79.7 \pm 1.4$	$87.2 \pm 1.5$
	$R_{--}$		$85.7 \pm 1.1$	$92.7 \pm 1.2$	$86.2 \pm 0.9$	$93.5 \pm 1$	$81.3 \pm 1.1$	$87.5 \pm 1.2$	$84.5 \pm 1.3$	$91.8 \pm 1.4$
			correlation function		correlation function		correlation function		correlation function	
		$86.2 \pm 1$	$93.3 \pm 1.1$	$84.8 \pm 1$	$92.9 \pm 1.1$	$79.3 \pm 0.9$	$85.8 \pm 1$	$82.1 \pm 1.3$	$88.9 \pm 1.3$	
1/frequency [a.u.]	exp		$21.5 \pm 0.05$	$21.5 \pm 0.05$	$43 \pm 0.3$	$43.3 \pm 0.3$	$43.9 \pm 0.26$	$43.9 \pm 0.25$	$14.4 \pm 0.04$	$14.4 \pm 0.04$
	calc						43	42.7	14.4	14.4
Bell parameter	S		$2.44 \pm 0.03$	$2.64 \pm 0.03$	$2.4 \pm 0.03$	$2.63 \pm 0.03$	$2.24 \pm 0.03$	$2.43 \pm 0.03$	$2.32 \pm 0.04$	$2.51 \pm 0.04$
	violation [σ]		15.5	20.5	14.1	20.2	9.6	15.1	8.8	14

TABLE I. Results for the experiment with simultaneous phase-change in both interferometers (see also table II and Fig. 3).

single counts [kHz]		dark	raw	net
	$D1+$	25.5	38.3	12.8
	$D1-$	25.5	37.4	11.9
	$D2+$	25.5	37.8	12.3
	$D2-$	25.5	37.9	12.4
measurement interval [s]	20			
window width [ps]	350			

TABLE II. Single count rates, measurement interval and window width for the experiment with simultaneous phase-change in both interferometers (see also table I and Fig. 3).

Scan in	Bellevue			Bernex			
		raw	netto		raw	netto	
single counts [kHz]	dark	light		dark	light		
	$D1+$	25.4	39.5	14.1	22.9	34.5	11.6
	$D1-$	25.3	38.6	13.3	23.5	34.3	10.8
	$D2+$	26.7	38.6	11.9	23.1	36.4	13.3
$D2-$	26.7	41	14.3	23.1	36.4	13.3	
measurement interval [s]		30			30		
window width [ps]		550			450		
coincidence counts	accidental	mean value		accidental	mean value		
	$R++$	$29 \pm 2.4$	$221.8 \pm 1.2$	$192.8 \pm 2.7$	$18.2 \pm 1.4$	$187.6 \pm 0.9$	$169.4 \pm 1.7$
	$R+-$	$25.6 \pm 2.3$	$285.7 \pm 1.3$	$260.2 \pm 2.7$	$16.6 \pm 1.3$	$210.8 \pm 1$	$194.2 \pm 1.7$
	$R-+$	$25.4 \pm 2.3$	$186.9 \pm 1.1$	$161.5 \pm 2.6$	$17.2 \pm 1.3$	$192.3 \pm 0.9$	$175.1 \pm 1.7$
$R--$	$25.8 \pm 2.3$	$254.1 \pm 1.3$	$228.3 \pm 2.7$	$21.2 \pm 1.5$	$209.8 \pm 1$	$188.6 \pm 1.8$	
visibilities	coincidence functions			coincidence functions			
	$R++$		$85.1 \pm 0.5$	$98 \pm 0.6$		$82.4 \pm 0.6$	$91.3 \pm 0.6$
	$R+-$		$87.9 \pm 0.5$	$96.6 \pm 0.5$		$83.4 \pm 0.5$	$90.5 \pm 0.6$
	$R-+$		$85.1 \pm 0.6$	$98.5 \pm 0.7$		$82 \pm 0.6$	$90.1 \pm 0.6$
	$R--$		$85.6 \pm 0.5$	$95.3 \pm 0.6$		$82.6 \pm 0.5$	$92.2 \pm 0.6$
	correlation function			correlation function			
	$l_c$		$83.7 \pm 0.5$	$93.6 \pm 0.5$		$81.1 \pm 0.4$	$88.8 \pm 0.5$
$2x\lambda$		$85.3 \pm 0.9$	$95.5 \pm 1$		$79.3 \pm 1.2$	$87.1 \pm 1.3$	
Bell parameter	S ( $2x\lambda$ )		$2.41 \pm 0.03$	$2.7 \pm 0.03$		$2.24 \pm 0.03$	$2.46 \pm 0.04$
	violation [ $\sigma$ ]		16.2	24.8		7.2	12.6

TABLE III. Results for the experiments with large phase changes in Bellevue and Bernex, respectively (see also Fig. 4.). The visibility " $l_c$ " denotes the visibility of the correlation function for a fit over a whole coherence length (including the gaussian envelope), " $2x\lambda$ " the one for a fit over only two periods. The Bell parameter S is given only for the last mentioned fit.

single counts [kHz]			raw	netto
		dark	light	
	$D_1$	25	30	5
	$D_1'$	25	29	4
	$D_{2+}$	25	36	11
	$D_{2-}$	25	36	11
measurement interval [s]		50		
window width [ps]		450		
coincidence counts		accidental	mean value	
	$R_{1+}$	$23.2 \pm 2$	$126.7 \pm 1.8$	$103.5 \pm 2.7$
	$R_{1-}$	$21.2 \pm 1.9$	$118 \pm 1.7$	$96.8 \pm 2.5$
	$R_{1'+}$	$19.2 \pm 1.8$	$94.5 \pm 1.4$	$75.3 \pm 2.3$
	$R_{1'-}$	$20 \pm 1.8$	$100.3 \pm 1.5$	$80.3 \pm 2.3$
visibilities			coincidence functions	
	$d_1$		$78.9 \pm 2$	$96 \pm 2.3$
	$d_1'$		$76.3 \pm 2.2$	$95.2 \pm 2.7$
x0	$d_1$		$786.4 \pm 0.1$	$786.4 \pm 0.1$
	$d_1'$		$791.6 \pm 0.1$	$791.6 \pm 0.1$
1/frequency [a.u.]	$d_1$		$23.5 \pm 0.1$	$23.5 \pm 0.1$
	$d_1'$		$23.5 \pm 0.1$	$23.5 \pm 0.1$
Bell parameter			indicated points	
	S		$2.38 \pm 0.16$	$2.92 \pm 0.18$
	violation [ $\sigma$ ]		2.4	5.1
			fit	
	S		$2.186 \pm 0.033$	$2.692 \pm 0.038$
	violation [ $\sigma$ ]		5.6	18.2

TABLE IV. Results for the experiment with three interferometers (see also Fig. 5).

single counts [kHz]			raw	netto
		dark	light	
	$D_1$	22.8	46	23.2
	$D_2$	22.5	39.8	17.3
	$D_3$	22.8	43.5	20.7
	$D_4$	23	50.8	27.8
measurement interval [s]		10		
window width [ps]		450		
coincidence counts		accidental	mean value	
	$R_{13}$	$9.3 \pm 0.9$	$103.7 \pm 0.9$	$94.4 \pm 1.3$
	$R_{24}$	$10.1 \pm 0.9$	$142.9 \pm 1$	$133 \pm 1.3$
	$R_{23}$	$8.2 \pm 0.8$	$84.5 \pm 1$	$79 \pm 1.6$
	$R_{24}$	$10 \pm 0.9$	$129.4 \pm 1.5$	$119.4 \pm 1.6$
visibilities			coincidence functions	
	$R_{13}$		$86.8 \pm 1.5$	$95.2 \pm 1.8$
	$R_{24}$		$85.6 \pm 1.2$	$92.2 \pm 1.3$
	$R_{23}$		$87.6 \pm 1.8$	$92.5 \pm 2.4$
	$R_{24}$		$80.5 \pm 1.6$	$87.9 \pm 1.8$
x0	$R_{13}$		$567.2 \pm 0.1$	$567.2 \pm 0.1$
	$R_{24}$		$557.1 \pm 0.1$	$557.1 \pm 0.1$
	$R_{23}$		$547 \pm 0.4$	$547.7 \pm 0.4$
	$R_{24}$		$568.5 \pm 0.3$	$568.5 \pm 0.3$
1/frequency [a.u.]	$R_{13}$		$39.2 \pm 0.1$	$39.2 \pm 0.1$
	$R_{24}$		$39.1 \pm 0.1$	$39 \pm 0.1$
	$R_{23}$		$85.6 \pm 0.9$	$82.8 \pm 1.3$
	$R_{24}$		$86.3 \pm 1$	$85.7 \pm 1$
Bell parameter			indicated points	
	S		$2.41 \pm 0.08$	$2.63 \pm 0.08$
	violation [ $\sigma$ ]		5.1	7.5
			fit	
	S		$2.45 \pm 0.03$	$2.66 \pm 0.03$
	violation [ $\sigma$ ]		14.5	22

TABLE V. Results for the experiment with four interferometers (see also Fig. 6 and 7).